Journal of Structural Biology 173 (2011) 138–145

Contents lists available at ScienceDirect

Journal of Structural Biology

journal homepage: www.elsevier.com/locate/yjsbi

Native architecture of the photosynthetic membrane from *Rhodobacter veldkampii*

Lu-Ning Liu [a], James N. Sturgis [b], Simon Scheuring [a,*]

[a] Institut Curie, U1006 INSERM, UMR168 CNRS, 26 Rue d'Ulm, 75248 Paris, France
[b] LISM CNRS, Aix Marseille Université, 31 Chemin Joseph Aiguier, 13402 Marseille, France

ARTICLE INFO

Article history:
Received 1 June 2010
Received in revised form 18 August 2010
Accepted 19 August 2010
Available online 24 August 2010

Keywords:
Atomic force microscopy
Membrane curvature
Membrane protein
Photosynthesis
PufX
Supramolecular organization

ABSTRACT

The photosynthetic membrane in purple bacteria contains several pigment–protein complexes that assure light capture and establishment of the chemiosmotic gradient. The bioenergetic tasks of the photosynthetic membrane require the strong interaction between these various complexes. In the present work, we acquired the first images of the native outer membrane architecture and the supramolecular organization of the photosynthetic apparatus in vesicular chromatophores of *Rhodobacter* (*Rb.*) *veldkampii*. Mixed with LH2 (light-harvesting complex 2) rings, the PufX-containing LH1–RC (light-harvesting complex 1 – reaction center) core complexes appear as C-shaped monomers, with random orientations in the photosynthetic membrane. Within the LH1 fence surrounding the RC, a remarkable gap that is probably occupied (or partially occupied) by PufX is visualized. Sequence alignment revealed that one specific region in PufX may be essential for PufX-induced core dimerization. In this region of ten amino acids in length all *Rhodobacter* species had five conserved amino acids, with the exception of *Rb. veldkampii*. Our findings provide direct evidence that the presence of PufX in *Rb. veldkampii* does not directly govern the dimerization of LH1–RC core complexes in the native membrane. It is indicated, furthermore, that the high membrane curvature of *Rb. veldkampii* chromatophores (*Rb. veldkampii* features equally small vesicular chromatophores alike *Rb. sphaeroides*) is not due to membrane bending induced by dimeric RC–LH1–PufX cores, as it has been proposed in *Rb. sphaeroides*.

1. Introduction

Photosynthesis is an important biological process performed by plants, algae and some bacteria. In purple bacteria, photosynthesis requires the high connectivity between several different membrane protein complexes: the peripheral light-harvesting complex 2 (LH2), the central light-harvesting complex 1 (LH1), the photochemical reaction center (RC) and a proton translocating cytochrome (cyt) *bc*1 complex that converts the energy into an electrochemical potential gradient, as well as the ATP synthase which is able to convert the energy into a phosphodiester bond of ATP (Cogdell et al., 2006; Hu et al., 2002). Most of these pigment–protein complexes are housed in specialized intracytoplasmic membranes (ICMs).

Much effort has been made to explore the architecture of photosynthetic complexes. In spite of the structural information of individual photosynthetic components, knowledge of the macromolecular organization of these protein complexes in the native state required for understanding the physiological activities and functional cooperativity of the photosynthetic apparatus awaited the dawn of atomic force microscopy (AFM). AFM with high lateral resolution and high signal-to-noise ratio has evolved into a powerful tool to directly and precisely visualize biological samples under physiological conditions (Engel and Gaub, 2008; Gonçalves and Scheuring, 2006; Scheuring, 2006). To date, AFM has significantly advanced the elucidation of the native surface views of ICMs from different photosynthetic bacteria, including lamellar discs in *Blastochloris* (*Blc.*) *viridis* (Scheuring et al., 2003a), *Rhodospirillum* (*Rsp.*) *photometricum* (Scheuring and Sturgis, 2005; Scheuring et al., 2004a,b) and *Rhodopseudomonas* (*Rps.*) *palustris* (Scheuring et al., 2006); vesicular structures in *Phaeospirillum* (*Phs.*) *molischianum* (Gonçalves et al., 2005a), *Rhodobacter* (*Rb.*) *sphaeroides* (Bahatyrova et al., 2004) and *Rb. blasticus* (Scheuring et al., 2005). These works unveiled the organization and dense packing of photosynthetic complexes, with a considerable mixing of peripheral LH2 and LH1–RC cores. The localization of the cyt bc_1 complex remains so far enigmatic, though evidence has been presented for the existence of pathways around the photosynthetic core complexes that may favor rapid quinone diffusion to distant cyt bc_1 complexes (Liu et al., 2009). AFM data has also been exploited to build three-dimensional models of the photosynthetic unit (Scheuring et al., 2007a; Şener et al., 2007), and various strategies that purple bacteria have evolved for the harvesting and utilization of light energy have been reviewed (Sturgis and Niederman, 2008).

Abbreviations: AFM, atomic force microscopy; EM, electron microscopy; ICM, intracytoplasmic membrane; LH, light-harvesting; OM, outer membrane; RC, reaction center.

* Corresponding author. Fax: +33 1 40510636.
E-mail address: simon.scheuring@curie.fr (S. Scheuring).

1047-8477/$ - see front matter © 2010 Elsevier Inc. All rights reserved.
doi:10.1016/j.jsb.2010.08.010

The core complex is the last complex of which a high-resolution structure is lacking, and its architecture varies between species (for review see Scheuring, 2006). It is composed of a central RC surrounded by LH1 subunits. The quinone is reduced in the Q_B site of the RC, followed by the diffusion across the LH1 ring and through the densely packed membrane to the cyt bc_1 complex. Besides the RC and LH1 an additional subunit, PufX, has been found to interact with the LH1–RC core complexes in *Rhodobacter* species studied (for review see Holden-Dye et al., 2008). It is a single transmembrane helix associated with the α-polypeptide of LH1 (Recchia et al., 1998). The presence of PufX has been speculated to play key roles in the dimerization of the core complex (Francia et al., 1999; Qian et al., 2005; Scheuring et al., 2005, 2004c). It was also proposed to be able to facilitate the quinone diffusion between RC and cyt bc_1 by opening the LH1 assembly around the RC (Francia et al., 1999; Qian et al., 2005).

In some *Rhodobacter* species the LH1–RC cores form dimers (Qian et al., 2005; Scheuring et al., 2005; Siebert et al., 2004), evidenced to align in rows interconnected by LH2 rings (Bahatyrova et al., 2004). These species feature vesicular ICMs (Oelze and Drews, 1972). It has therefore been advanced that the ICM shape is governed by the organization and interaction of the integral membrane proteins (Hunter et al., 2005; Jungas et al., 1999; Olsen et al., 2008), in particular the bending of S-shaped RC–LH1–PufX core dimers (Chandler et al., 2008; Hsin et al., 2009b; Qian et al., 2008; Scheuring et al., 2004c).

Phylogenetic analysis on the basis of the 16S RNA sequence revealed that *Rb. veldkampii* has diverged from other *Rhodobacter* species, for example *Rb. sphaeroides*, *Rb. blasticus*, *Rb. capsulatus* and *Rb. azotoformans* (Tsukatani et al., 2004). The detergent solubilized and biochemically isolated photosynthetic complexes of *Rb. veldkampii* have been examined and monomeric RC–LH1–PufX core complexes with two species of LH2 complexes were found (Busselez et al., 2007; Gubellini et al., 2006). However, one may argue whether the core complexes form monomers *in vivo*, or whether the association of dimeric cores in *Rb. veldkampii* is too weak to maintain the dimeric core architecture during isolation in the presence of detergent. Furthermore, if core dimerization induces membrane bending (Qian et al., 2008), what ICM morphology appears in *Rb. veldkampii*?

To address these questions, here we report the first characterization of the native architecture of the photosynthetic membrane from *Rb. veldkampii*. In the vesicular ICM, we observe the RC–LH1–PufX core complex monomers besides LH2 rings. The RC is surrounded by a C-shaped LH1 assembly and a remarkable gap assigned to the putative position of PufX protein. The physiological significance of PufX in the dimerization of LH1–RC core complexes and the roles of RC–LH1–PufX monomer in membrane curvature are discussed. Our findings question the current view of core-dimer-induced ICM morphology and identify a sequence stretch in PufX that might be responsible for core monomer or dimer association states.

2. Material and methods

2.1. Bacterial culture, membrane preparation and optical absorbance spectroscopy

Rb. veldkampii strain DSM11550 (German Strain Collection of Microorganisms and Cell Culture, DSMZ, Braunschweig, Germany) was grown for 72 h (OD_{670} = 4 AU) under photosynthetic conditions (Busselez et al., 2007). Membranes were prepared as previously described (Francia et al., 1999). Briefly, cells were disrupted with a French press and centrifuged to remove cell debris. Supernatant was ultracentrifuged in a Beckman Ti45 rotor for 90 min at 125,000*g* (4 °C), and the resulting membrane pellet was resuspended in 50 mM glygly (pH 7.8), 1 mM EDTA, and 1 mM benzoamidine (Busselez et al., 2007; Gubellini et al., 2006). The membranes containing mainly photosynthetic membranes and some outer membrane fragments were then kept at 4 °C for AFM analysis. Absorption spectra were recorded at room temperature by a Lambda 800 spectrophotometer (PerkinElmer, USA) using a 1-cm pathway cuvette with a bandwidth of 2 nm.

2.2. Transmission electron microscopy

Cell samples for transmission electron microscopy (EM) were fixed, stained, and sectioned as described before (Hunter et al., 1988), and then examined on a Zeiss EM 109 transmission electron microscope at 80 kV.

2.3. Atomic force microscopy

A Nanoscope-E AFM (Binnig et al., 1986) (Veeco, Santa Barbara, CA, USA), equipped with a 160-μm scanner (J-scanner) and oxide-sharpened Si_3N_4 cantilevers (length 100 μm; k = 0.09 N/m; Olympus Ltd., Tokyo, Japan) was operated in contact mode at ambient temperature and pressure. For imaging minimal loading forces of ~100 pN were applied, at scan frequencies of 4–7 Hz using optimized feedback parameters. The mica supports were immerged in 40 μL adsorption buffer (10 mM Tris–HCl, pH 7.5, 150 mM KCl, 25 mM $MgCl_2$). Subsequently, 2 μL of membrane solution were injected into the buffer drop. After ~1 h the sample was rinsed with recording buffer (10 mM Tris–HCl, pH 7.5, 150 mM KCl) before imaging.

2.4. Data analysis

AFM images were flattened and analyzed using Veeco Nanoscope software. Core complexes were analyzed as in previous works on non-symmetric core complexes (Scheuring et al., 2006, 2003a). The LH1 ellipticity was analyzed on the protrusion top of individual LH1 complexes observed. The ellipsis value is independent on the gap location by the best fit of an ellipsis to the part of the ring that is visible (Scheuring et al., 2003a). Particle averaging was performed using cross-correlation based Java routines for the ImageJ image processing package (Fechner et al., 2009; Rasband, 1997–2005; Saxton and Baumeister, 1982; Scheuring et al., 2007b). Sequence alignment was performed using ClustalX based on amino acid sequences of the PufX in five species, *Rb. veldkampii* (GI:51971305), *Rb. capsulatus* (GI:294676252), *Rb. blasticus* (GI:51971303), *Rb. sphaeroides* (GI:77463824), *Rb. azotoformans* (GI:51971301). The X-ray structure of the extracellular side of OM porins from *Rb. blasticus* (PDB: 2POR) was rendered in molecular surface representation with PyMol (DeLano, 2002) for comparison with the AFM topographs of OM porins from *Rb. veldkampii*.

3. Results

3.1. Cell and chromatophore morphology

In order to study the morphologies of the cells and ICMs *in vivo*, thin sections of whole cells were examined in an electron microscope. As depicted in Fig. 1A, *Rb. veldkampii* cells appear to be ovoid, 0.5–0.8 μm wide and 1.0–1.3 μm long, consistent with the previous description (Hansen et al., 1975). Besides the outer membrane (OM) and the cytoplasmic membrane of the cell, the internal photosynthetic membranes of *Rb. veldkampii* were visualized as vesicles with an average diameter of about 50 nm, comparable to those in *Rb. sphaeroides* (Hunter et al., 1988; Sturgis and Niedermann, 1996).

The photosynthetic membranes from *Rb. veldkampii* were prepared by French pressure cell breaking and gentle purification by

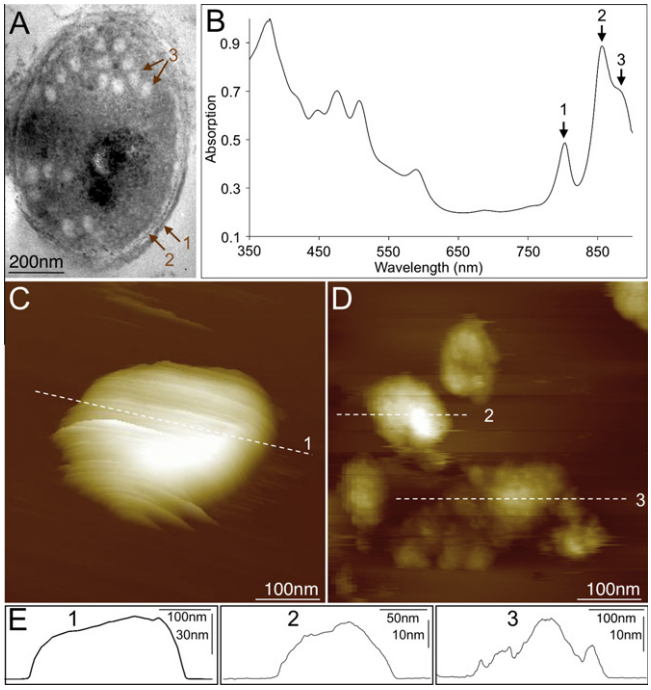

Fig. 1. *Rb. veldkampii* cell and chromatophores. (A) Thin-section electron micrograph depicting the membranes structure and the ICM architecture and distribution in a *Rb. veldkampii* cell: (1) outer membrane; (2) cytoplasmic membrane; (3) vesicular ICMs. (B) Room-temperature absorption spectrum of isolated photosynthetic membranes from *Rb. veldkampii*. The arrows show the near-infrared absorption bands of LH2 at 803 nm (1) and 856 nm (2), and LH1 at 880 nm (3). (C) Vesicular ICM absorbed on mica support. (D) AFM image of photosynthetic membrane fragments. (E) Cross-section analysis along the dashed lines in (C) and (D).

ultracentrifugation in absence of any detergent throughout the treatment (see Section 2). The absorption spectrum of isolated ICMs is shown in Fig. 1B. The absorption maxima at 372, 448, 476, 508, 589 nm indicated the presence of bacteriochlorophyll *a* and carotenoids. Absorption maxima at 803 nm and 856 nm are attributed to the bacteriochlorophylls in LH2; the 880-nm shoulder band arises mainly from LH1, consistent with the previous results (Hansen and Imhoff, 1985).

Importantly, gently prepared ICMs preserved their vesicular shape in the AFM (Fig. 1C). ICM vesicles were imaged with a height of ~50 nm and a width of ~200 nm. We found high-resolution images of the photosynthetic apparatus were somehow difficult to acquire on such vesicles compared to sheet-like membranes as for example found in *Rsp. photometricum*. This is probably due to the softness of the vesicle eventually inferior to the spring constant of the cantilever, but also because the intact vesicles do not firmly attach to the mica surface. However, at minimal loading force there is still possibility that the morphological features of the vesicles and embedded proteins can be imaged (Fig. 1D). The cross-section analysis showed the vesicular profiles of the ICMs (Fig. 1E).

3.2. Native organization and architecture of the photosynthetic apparatus

Closer examination using AFM gave an overview of the distributions of LH2 and core complexes in the photosynthetic membranes (Fig. 2). Upon high-magnification image acquisition, the vesicles appeared flattened, most likely due to higher effective loading forces when scanning small surface areas. The first AFM images of the native photosynthetic membrane from *Rb. veldkampii* clearly display that LH2 and core complexes had no significant order within the membrane. The membranes contain a mixture of randomly arranged LH1–RC cores and circular LH2 rings at a ratio of about 1:2.6. The core complexes appear as monomers and are randomly oriented with respect to each other. In some areas, core complexes are seen in contact, and such connectivity may increase the probability for excitons to find a functional "open" RC, thus enhancing rapid energy trapping. This arrangement is comparable to that seen in *Rsp. photometricum*, *Phsp. molischianum*, and *Rps. palustris* (Liu et al., 2009; Scheuring and Sturgis, 2005; Scheuring et al., 2006).

The top ring diameter of LH2 complexes is 51 ± 2 Å (mean ± standard deviation, $n = 30$), in size agreement with the nonameric ring of LH2 complexes (Scheuring et al., 2004a, 2006) (Fig. 3). In addition, our AFM images also show a few LH-like proteins present a larger size (Fig. 3, arrows) in contrast to the majority of LH2 complexes. This could explain the previous observation about two distinct LH2 complex species of significantly different size found in sucrose gradients (Gubellini et al., 2006). Variability of LH2 complexes with 8mer (~10%), 9mer (~80%) and 10mer (~10%) symmetry has been seen in *Rsp. photometricum* at high-resolution, with very rare antenna complexes that had a size of about 80 Å in diameter bearing between 12 and 14 LH subunits (Scheuring and Sturgis, 2005; Scheuring et al., 2004a).

Rb. veldkampii and *Rb. sphaeroides* both contain vesicular chromatophores, the organization of the photosynthetic apparatus within these two organisms is however different. The most significant difference is the architecture of core complexes: monomer in *Rb. veldkampii* and dimer in *Rb. sphaeroides* (Table 1). Although we

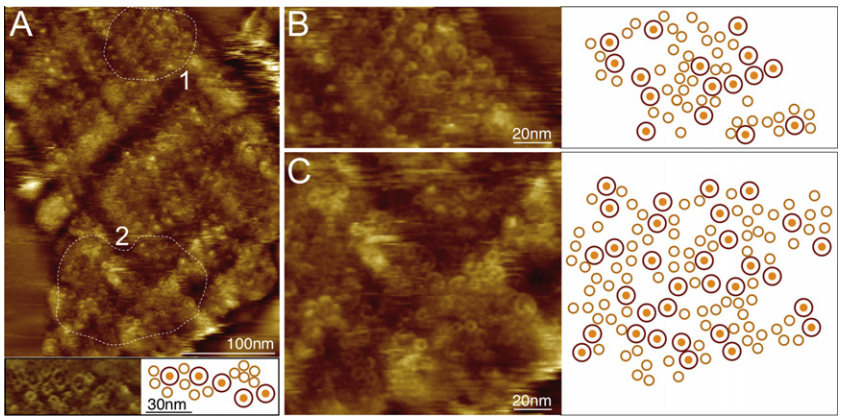

Fig. 2. AFM analysis of the photosynthetic apparatus from *Rb. veldkampii*. (A) Medium resolution topograph. Inset, the organization of the photosynthetic apparatus and schematic model. (B) and (C) Closer views of the membrane regions marked by broken lines 1 and 2, respectively in (A), showing the overview distributions of LH2 and core complexes as depicted by schematic model.

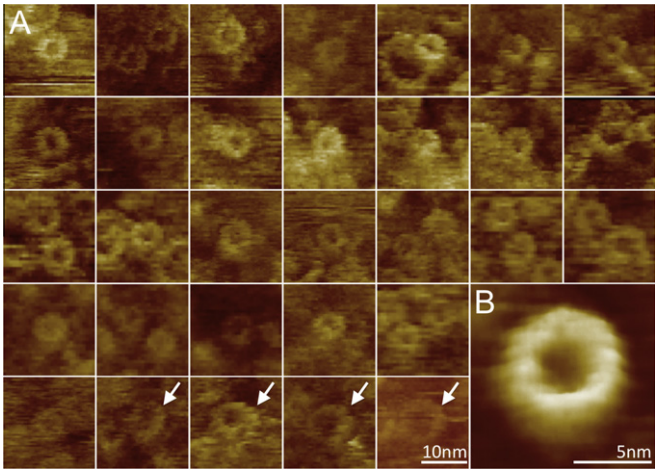

Fig. 3. The structures of LH2 complexes in *Rb. veldkampii* membranes. (A) LH2 complexes in AFM topographs. Note that some LH-like complexes (arrows) present larger size than others, probably corresponding to the second enlarged LH2 type found in *Rb. veldkampii* (Gubellini et al., 2006). (B) Average of the normal sized LH2 complexes ($n = 30$). The top ring diameter is 51 ± 2 Å, in size agreement with ninefold symmetrical LH2 (Scheuring et al., 2004a, 2006).

found the membrane surface is highly corrugated, high-resolution images of the photosynthetic apparatus from *Rb. veldkampii* could still be acquired. As depicted in Fig. 4A and B, the core complex of *Rb. veldkampii* is in the monomeric state, consisting of a RC surrounded by LH1 subunits. In addition, a gap within the LH1 assembly was observed.

High-resolution images showed well-defined core complex (Fig. 4C). In the monomeric core complex, the central RC is surrounded by a total of 15 α/β heterodimers (labeled 1–15) (Fig. 4C left). Actually due to the irregular membrane surface, not all individual LH1 subunits can be clearly visualized and their subunit number determined (Fig. 4C middle and right), in spite of the fact that structural heterogeneity might occur *in vivo*. The core complexes have an elliptical shape with an axis ratio of 1.15 (105 ± 6 Å and 91 ± 5 Å, $n = 44$, measured from protrusion top to protrusion top of the LH1) (Table 1), with the long axis following the RC orientation (Fig. 4C, cyano arrows). This resembles the core complex of *Rps. palustris* (axes ratio: 1.18) (Scheuring et al., 2006). Interestingly, the protein-free gap in the LH1 cylinder, putative molecular localization of the PufX peptide, has an opening distance of 62 ± 5 Å (measured between the inner edges at both ends of the C-shaped LH1 assembly), larger than the space observed in single particle EM study (40 Å) (Busselez et al., 2007). This C-shaped RC–LH1–PufX core complexes is reminiscent of the structure of monomeric cores arising from broken dimers in *Rb. blasticus* (Scheuring et al., 2005). Such an enlarged gap might favor the migration of quinone and quinol molecules passage in and out of the LH1 boundary between RC–LH1–PufX cores and physically distant cyt bc_1 complexes, though its physiological importance remains to be further explored, because many species function with complete LH1 rings around the RC (Scheuring, 2006). We have recently described quinone pathways in *Rsp. photometricum* chromatophores (Liu et al., 2009), and similar quinone pathways might exist in vesicular ICMs such as in *Rb. veldkampii* or *Rb. sphaeroides*.

Besides the LH1 ellipticity, the structural variability of core complexes is also explored (Fig. 5). In addition to the above-described C-shaped structure, some LH1 of the cores among the 44 core complexes investigated in detail in this work seem almost closed. Indeed, 84% of the cores feature an "open" LH1 assembly ($n = 37$) while 16% appear rather "closed" ($n = 7$). Due to the high signal-to-noise ratio and the capacity to study individual proteins, the AFM is currently the only technique that is able to detect the protein structural variability at the individual molecule level (Scheuring and Sturgis, 2009). Moreover, the gap in the LH1 fence could be seen at the periapsis or at the apoapsis of the LH1 ellipsoid, coinciding with the findings of *Rps. palustris* core complex structure (Scheuring et al., 2006).

3.3. The PufX polypeptide

The *pufX* gene has been identified in five *Rhodobacter* species, *Rb. sphaeroides*, *Rb. azotoformans*, *Rb. capsulatus*, *Rb. blasticus* and *Rb. veldkampii* (Tsukatani et al., 2004). Fig. 6A exhibits the sequence alignment (based on Tsukatani et al., 2004) of the PufX peptides from the five species. The PufX sequences do not present

Table 1
Structural comparison of the LH1–RC core complex of *Rb. veldkampii*, and of other species investigated.

Species	Sample	Technique	Monomer/dimer	PufX (W) location	α/β pairs	Long axis (Å)	Short axis (Å)	Ratio	Gap (Å)	Reference
Rb. veldkampii	Native membrane	AFM	Monomer	Gap[a]	15	105 ± 6	91 ± 5	1.15	62 ± 5	In this work
	Isolated protein	EM	Monomer	Gap[a]	15	133	129	1.03	40	Busselez et al., 2007
Rb. blasticus	Native membrane	AFM	Dimer	Dimer center	2 × 13	100	90	1.11	49	Scheuring et al., 2005
Rb. sphaeroides	Native membrane	EM	Dimer	–	2 × 12	112	112	1.00	30	Jungas et al., 1999
	Native membrane	AFM	Dimer	2 × palustris core complex		–	–	–	–	Bahatyrova et al., 2004
	2D crystal	EM	Dimer	LH1 "S" extremities	2 × 14	130	130	1.00	28	Qian et al., 2005
	2D crystal	EM	Dimer	Dimer center	2 × 12	110	110	1.00	28	Scheuring et al., 2004c
	2D crystal	EM	Dimer ($PufX^+$)	2 × palustris core complex		95	105	0.90	32	Siebert et al., 2004
	2D crystal	EM	Monomer ($PufX^-$)	–	–	105	105	1.00	0	Siebert et al., 2004
	2D crystal	EM	Monomer ($PufX^-$)	–	15–17	90	90	1.00	0	Walz et al., 1998
Rps. palustris (W)	Isolated protein	X-ray	Monomer	Gap	15	110	95	1.16	30	Roszak et al., 2003
	Native membrane	AFM	Monomer	Gap[a]	15	99	83	1.18	27	Scheuring et al., 2006
Rsp. photometricum	Native membrane	AFM	Monomer	–	16	95	85	1.12	0	Scheuring and Sturgis, 2005
Rsp. rubrum	2D crystal	EM	Monomer	–	16	115	109	1.06	0	Jamieson et al., 2002
	2D crystal	AFM	Monomer	–	16	130	110	1.18	0	Fotiadis et al., 2004
Blc. viridis	Native membrane	AFM	Monomer	–	16	104	98	1.06	0	Scheuring et al., 2003a
	Native membrane	EM	Monomer	–	12	120	120	1.00	0	Stark et al., 1984
Phs. molischianum	Native membrane	AFM	Monomer	–	16	95	85	1.12	0	Gonçalves et al., 2005a
	Isolated protein	EM	Monomer	–	12	110	110	1.00	0	Boonstra et al., 1994

[a] Attributed.

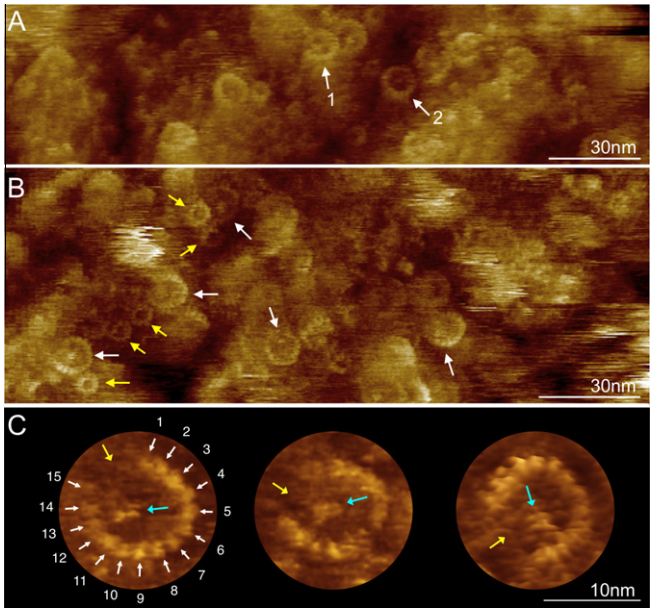

Fig. 4. Molecular resolution AFM images of the photosynthetic apparatus from *Rb. veldkampii*. (A) and (B) Supramolecular organization of the photosynthetic apparatus. Arrow 1 in (A) points out a C-shaped "open" LH1 assembly, whereas arrow two depicts a "closed" core complex. Core complexes are monomers (white arrows), and LH2 complexes (yellow arrows) are surrounding the cores. (C) High-resolution topographs showing the subunit architecture of three C-shaped RC–LH1–PufX core monomers. The RC is pointed out by cyan arrows, and the arrow direction is parallel to the long axis of RC. Fifteen well-characterized individual LH1 α/β heterodimers were visualized surrounding the RC, according to the topographic profiles of the LH1 fence and the averaged distance between individual α/β pairs. A gap attributed to the location of PufX within the LH1 assembly is depicted (yellow arrows). (For interpretation of the references in colour in this figure legend, the reader is referred to the web version of this article.)

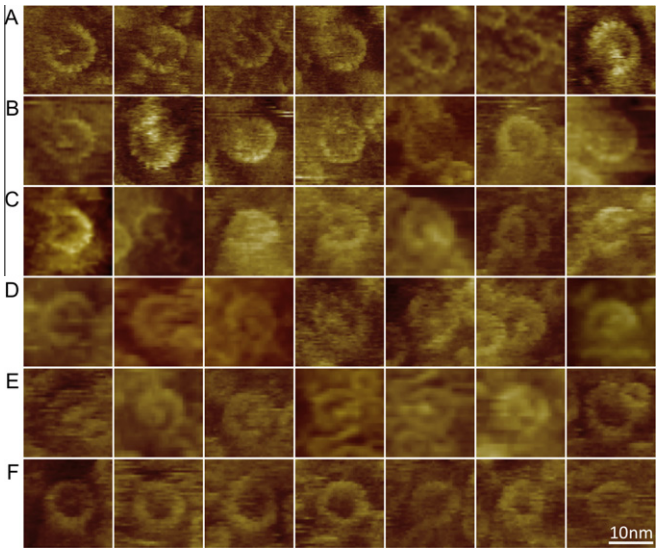

Fig. 5. The variability of RC–LH1–PufX monomeric core complexes in AFM topographs. (A) to (E) Core complexes with an "open" LH1 arrangement. (F) Core complexes that show a "closed" LH1 structure.

high identity, with the exception of two conserved clusters (WxxxQMxxGA and GxxLPxxxxxAPxP) at approximate positions 25 and 60 of a total of about 80 amino acids in length, including eight completely conserved amino acid residues of PufX in all five species (highlighted in red). The second cluster of six amino acids (G_{52}, L_{55}, P_{56}, A_{62}, P_{63}, P_{65}) at the C-terminal end of the transmembrane helix is absolutely conserved in all species. In contrast, the first cluster of five amino acids (W_{22}, Q_{26}, M_{27}, G_{30}, A_{31}) located almost in the center of the transmembrane helix is conserved in all species but not in *Rb. veldkampii*, in which W_{22} is altered to M_{22}, Q_{26} to A_{26}, and A_{31} to M_{31}. It was proposed previously that the glycine-rich GxxxG motif (highlighted in yellow in Fig. 6A) in the *Rb. sphaeroides* PufX may account for the ability of PufX to facilitate core complex dimerization (Busselez et al., 2007), and recent molecular dynamics simulations are favorable for the potential role of this motif (Hsin et al., 2009a). However, the sequence alignment in this work showed that this motif is only unique to *Rb. sphaeroides*, and not conserved in other *Rhodobacter* species that have dimeric cores, for instance *Rb. blasticus* (Scheuring et al., 2005). This implies that this motif is unlikely to be key in driving the formation of RC–LH1–PufX core dimers (Holden-Dye et al., 2008). As described above, we found alternatively strong deviation in the central membrane-spanning region of the *Rb. veldkampii* PufX sequence compared to those of other *Rhodobacter* species (WxxxQMxxGA). The cluster QMxxGA in all other *Rhodobacter* species PufX is exposed to the same α-helix surface of about 36 $Å^2$ area in the solution NMR structure of PufX (Tunnicliffe et al., 2006; Wang et al., 2007) (Fig. 6B and C). We therefore propose that the motif WxxxQMxxGA of the PufX peptide is likely involved in core dimerization.

3.4. The outer membrane

The OM plays an essential role in protecting Gram-negative bacteria. Recently, the first high-resolution view of supramolecular assembly of porins in the OM of *Rosebacter* (*R.*) *denitrificans* has been reported (Jarosławski et al., 2009). To evaluate whether the observed OM morphology is general in different bacterial photosynthetic species, we further studied here the OM from *Rb. veldkampii*. The unique trimeric assembly of porins and the absence of photosynthetic complexes allow us to distinguish unambiguously the OM fragments from photosynthetic membrane vesicles. As shown in Fig. 7A, porins form a molecular sieve with a high packing density in the OM, consistent with the OM architecture found in *R. denitrificans* (Jarosławski et al., 2009). Each of the three monomers comprises a channel, a 16-stranded transmembrane β-barrel, which is connected by short turns on the periplasmic side and long loops on the extracellular side (Weiss and Schulz, 1992). Fig. 7B depicts the porins at molecular resolution viewed from the extracellular side with three major protrusions corresponding to the long loops connecting β-strands (Jarosławski et al., 2009; Müller and Engel, 1999; Schabert et al., 1995). The loops protruded of 5.6 ± 0.5 Å (n = 20) from the lipid bilayer surface, and were spaced by 48.0 ± 1.0 Å (n = 20) (Fig. 7C). These features are the typical characteristics of the extracellular surface of OM porins, resembling previous AFM observations of *Escherichia coli* OmpF in 2D crystals (Müller and Engel, 1999; Schabert et al., 1995), recent finding of OM in *R. denitrificans* (Jarosławski et al., 2009), and the surface representation of the atomic structure of protein from *Rb. capsulatus* (Fig. 7D, PDB code: 2POR).

4. Discussion

4.1. Core complex architecture

AFM topographs have revealed that the core complex architecture varied considerably between species (Scheuring, 2006). Table 1 showed that the core complex architectures of different bacterial photosynthetic organisms characterized by AFM, EM and X-ray crystallography. It was proposed that the PufX plays key roles in

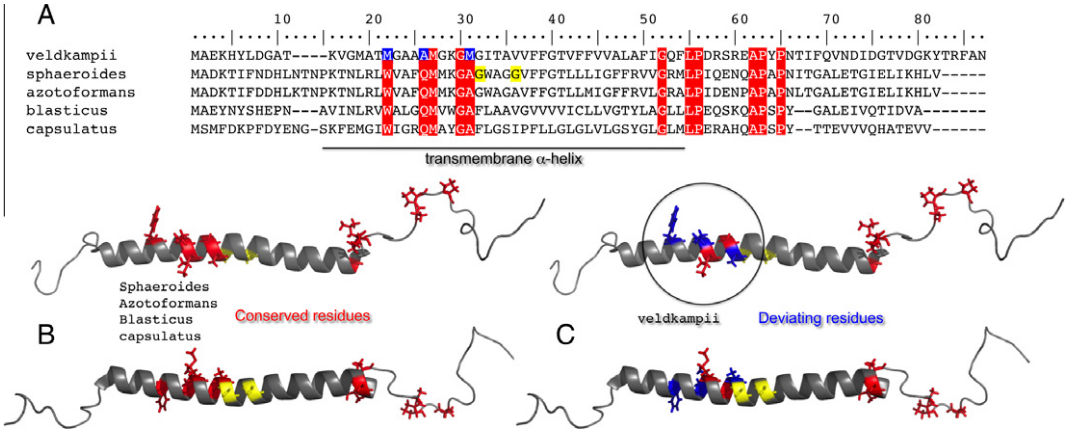

Fig. 6. Sequence and structure analysis of PufX peptides. (A) Sequence alignment of PufX of five *Rhodobacter* species, *Rb. veldkampii*, *Rb. sphaeroides*, *Rb. azotoformans*, *Rb. blasticus* and *Rb. capsulatus*. Highly conserved amino acid residues are highlighted in red. Residues conserved in all other four species but altered in *Rb. veldkampii* are highlighted in blue. The GxxxG motif in the *Rb. sphaeroides* PufX sequence, proposed to be critical for dimerization of core complexes is highlighted in yellow (Busselez et al., 2007). (B) and (C) 3D structure of the PufX of *Rb. sphaeroides* (PDB code: 2DW3) (Wang et al., 2007) viewed from two different angles (90° rotated with respect to each other). Amino acids conserved in *Rb. sphaeroides*, *Rb. azotoformans*, *Rb. blasticus*, *Rb. capsulatus* are shown in red (B), and the residues deviating from this preservation in *Rb. veldkampii* are colored in blue (C). The GxxxG motif is colored in yellow. (For interpretation of the references in colour in this figure legend, the reader is referred to the web version of this article.)

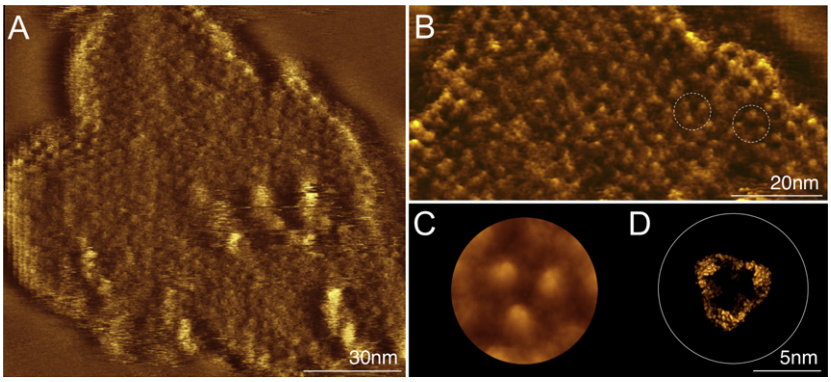

Fig. 7. AFM analysis of the OM of *Rb. veldkampii*. (A) Overview image of the extracellular surface of an OM fragment. (B) High-resolution image of the extracellular surface. The OM is densely packed with the major trimeric porins (dashed circles). (C) Threefold symmetrized porin average ($n = 20$). (D) Surface representation of the extracellular side of the porin from *Rb. capsulatus* represented by PyMol (PDB code: 2POR) (DeLano, 2002).

the core dimerization, and thus PufX-containing core complexes exist most likely in the dimeric state. Busselez et al. (2007) have shown, using purified core complexes, that in *Rb. veldkampii* RC–LH1–PufX core complexes are monomers (Busselez et al., 2007). Here, we consolidate this finding and ascertain further that this architecture is indeed present in the native membrane *in vivo*. However, AFM revealed structural heterogeneity of a minority of the RC–LH1–PufX core complexes in the native membrane.

Surprisingly, AFM images of the native photosynthetic membrane from *Rb. veldkampii* also showed a unique architecture of the RC–LH1–PufX core complexes, with a larger space of the LH1 gap in the core monomers compared to the core structure acquired in the isolated state (Busselez et al., 2007). The existence of the notable protein-free area in the native membrane environment might hint the potential function of lipid–protein interactions in maintaining the supramolecular architecture of the core complex. From the physiological point of view, this increased gating space might provide more open and flexible environment for quinone/quinol diffusion, and thus facilitate the communication with cyt bc_1 complexes.

Kinetics analysis of flash-induced cyt b_{561} reduction indicated that, the PufX favors the quinone-mediated redox interaction between the RC and cyt bc_1 complexes in the same manner in both *Rb. veldkampii* and *Rb. sphaeroides* (Gubellini et al., 2006). Obviously, though the sequence similarity of PufX peptides in different species is low, the protein can still sustain its physiological functions (Fulcher et al., 1998; Holden-Dye et al., 2008). It is interesting to observe that the RC–LH1–PufX core complexes are monomeric in the native membrane of *Rb. veldkampii*, whereas it is dimeric in *Rb. sphaeroides* (Bahatyrova et al., 2004; Scheuring et al., 2004c) and *Rb. blasticus* (Scheuring et al., 2005). Although structural information about the core complexes from *Rb. capsulatus* and *Rb. azotoformans* is still lacking, we conclude that dimerization of LH1–RC core complexes is not simply ascribed to the presence of PufX. Our sequence analysis, furthermore, pinpoints a specific amino acid domain (WxxxQMxxGA) in the central α-helical region of PufX, which may play an important role in the dimer association between PufX.

It is worthy to note that our AFM images did not reveal the position of the PufX in the core complex. With only one transmembrane helix, the topography of PufX would be minor in the lipid membrane. The enlarged space of the LH1 gap probably also raises the difficulty of PufX positioning. A high-resolution 3D structure of this C-shaped core complex is required to address this question.

4.2. The organization of the photosynthetic apparatus and membrane curvature

The ICMs present various morphologies depending on the species: stacked lamellar discs in *Rsp. photometricum*, *Phsp. molischianum* and *Rps. palustris*, whereas small vesicles in *Rb. sphaeroides* and *Rsp. rubrum* (Scheuring and Sturgis, 2009; Sturgis et al., 2009). It is generally accepted that membrane curvature is driven by membrane proteins involved in the chromatophores. Variation in the amount of one type of complex could also modulate the size of the vesicles (Sturgis and Niedermann, 1996).

LH2 complexes have been proposed to bend the membrane. First, tilt of LH2 barrels in 2D crystals has been observed by electron crystallography (Walz et al., 1998). The tilt of LH2 rings has been determined to be 6° with respect to the membrane normal (Scheuring et al., 2003b). Further studies have confirmed these findings (Liu et al., 2008; Olsen et al., 2008). However, these findings have little impact concerning the native membrane, as this behavior of LH2 complexes has been observed when reconstituted, often in up-and-down orientation, in non-natural lipids, at extremely low lipid-to-protein ratio, or under several of these non-native conditions. It was also shown that LH2 complexes can or cannot reveal tilt depending on the conditions (Gonçalves et al., 2005b). Computer simulation showed that specific arrays of LH2s, like seven hexagonally arranged domains, may drive the spherical curvature (Chandler et al., 2008, 2009). However, the assembly of LH2s and cores seems more random in the *Rb. veldkampii* membrane.

Regardless of whether LH2s are eventually found to curve the membrane or not, the dimeric cores were thought to play an essential role in the membrane curvature. Evidence for this is that in mutant ICMs from *Rb. sphaeroides* devoid of LH2, the RC–LH1–PufX dimers induce anisotropic curvature and form cylindrical membrane tubes (Hunter et al., 1988; Jungas et al., 1999; Qian et al., 2008). Single particle analysis of the dimeric core complex clearly showed a curved side-view profile (Qian et al., 2008). Molecular dynamics simulation, using a model structure derived from this study, indicated core dimers may drive membrane curvature (Chandler et al., 2008; Hsin et al., 2009b). However, the present study unambiguously shows that monomeric RC–LH1–PufX complexes can be present in vesicular ICMs in *Rb. veldkampii* comparable to the ICMs found in *Rb. sphaeroides*. This is direct evidence that the core dimerization is not prerequisite for the formation of vesicular chromatophores. Considering the fact that *Rb. veldkampii* (with LH2 and monomeric cores) features equally small vesicular chromatophores alike *Rb. sphaeroides* (with LH2 and dimeric cores), our results indicate that LH2 complexes might take the lead responsibility for the formation of vesicular chromatophores.

5. Conclusions

In the present work, using AFM we have observed the native organization of vesicular photosynthetic membrane and outer membrane from *Rb. veldkampii*. A specific C-shaped structure of the monomeric RC–LH1–PufX core complexes was characterized in the native vesicular ICM. Our data further reveals that one sequence cluster in the central transmembrane region of PufX is probably responsible for the core dimerization. Three amino acid residues in this cluster are unique in *Rb. veldkampii*, and thus lead to the formation of core monomers. The existence of RC–LH1–PufX monomeric core complexes in vesicular chromatophores has important implications for the membrane organization and curvature. It provides strong experimental evidence that the long-range membrane curvature in *Rb. veldkampii* is not driven by the RC–LH1–PufX core dimers. More detailed mechanisms of membrane curvature in photosynthetic bacteria remain to be further investigated.

Acknowledgments

The authors thank Dr. D. Lévy for the strain. This study was supported by the Institut Curie, the Institut National de la Santé et Recherche Médicale (INSERM), the Centre National de la Recherche Scientifique (CNRS), the Agence Nationale de la Recherche (ANR), and the 'City of Paris'.

References

Bahatyrova, S., Frese, R.N., Siebert, C.A., Olsen, J.D., van der Werf, K.O., van Grondelle, R., Niederman, R.A., Bullough, P.A., Otto, C., Hunter, C.N., 2004. The native architecture of a photosynthetic membrane. Nature 430, 1058–1062.

Binnig, G., Quate, C.F., Gerber, C., 1986. Atomic force microscope. Phys. Rev. Lett. 56, 930–933.

Boonstra, A.F., Germeroth, L., Boekema, E.J., 1994. Structure of the light harvesting antenna from *Rhodospirillum molischianum* studied by electron microscopy. Biochim. Biophys. Acta. 1184, 227–234.

Busselez, J., Cottevieille, M., Cuniasse, P., Gubellini, F., Boisset, N., Lévy, D., 2007. Structural basis for the PufX-mediated dimerization of bacterial photosynthetic core complexes. Structure 15, 1674–1683.

Chandler, D.E., Hsin, J., Harrison, C.B., Gumbart, J., Schulten, K., 2008. Intrinsic curvature properties of photosynthetic proteins in chromatophores. Biophys. J. 95, 2822–2836.

Chandler, D.E., Gumbart, J., Stack, J.D., Chipot, C., Schulten, K., 2009. Membrane curvature induced by aggregates of LH2s and monomeric LH1s. Biophys. J. 97, 2978–2984.

Cogdell, R.J., Gall, A., Köhler, J., 2006. The architecture and function of the light-harvesting apparatus of purple bacteria: from single molecules to in vivo membranes. Q. Rev. Biophys. 39, 227–324.

DeLano, W.L., 2002. The PyMOL Molecular Graphics System. DeLano Scientific, Palo Alto, CA, USA. http://www.pymol.org.

Engel, A., Gaub, H.E., 2008. Structure and mechanics of membrane proteins. Annu. Rev. Biochem. 77, 127–148.

Fechner, P., Boudier, T., Mangenot, S., Jarosławski, S., Sturgis, J.N., Scheuring, S., 2009. Structural information, resolution, and noise in high-resolution atomic force microscopy topographs. Biophys. J. 96, 3822–3831.

Fotiadis, D., Qian, P., Philippsen, A., Bullough, P.A., Engel, A., Hunter, C.N., 2004. Structural analysis of the reaction center light-harvesting complex I photosynthetic core complex of *Rhodospirillum rubrum* using atomic force microscopy. J. Biol. Chem. 279, 2063–2068.

Francia, F., Wang, J., Venturoli, G., Melandri, B.A., Barz, W.P., Oesterhelt, D., 1999. The reaction center-LH1 antenna complex of *Rhodobacter sphaeroides* contains one PufX molecule which is involved in dimerization of this complex. Biochemistry 38, 6834–6845.

Fulcher, T.K., Beatty, J.T., Jones, M.R., 1998. Demonstration of the key role played by the PufX protein in the functional and structural organization of native and hybrid bacterial photosynthetic core complexes. J. Bacteriol. 180, 642–646.

Gonçalves, R.P., Scheuring, S., 2006. Manipulating and imaging individual membrane proteins by AFM. Surf. Interface Anal. 38, 1413–1418.

Gonçalves, R.P., Bernadac, A., Sturgis, J.N., Scheuring, S., 2005a. Architecture of the native photosynthetic apparatus of *Phaeospirillum molischianum*. J. Struct. Biol. 152, 221–228.

Gonçalves, R.P., Busselez, J., Lévy, D., Seguin, J., Scheuring, S., 2005b. Membrane insertion of *Rhodopseudomonas acidophila* light harvesting complex 2 investigated by high resolution AFM. J. Struct. Biol. 149, 79–86.

Gubellini, F., Francia, F., Busselez, J., Venturoli, G., Lévy, D., 2006. Functional and structural analysis of the photosynthetic apparatus of *Rhodobacter veldkampii*. Biochemistry 45, 10512–10520.

Hansen, T.A., Imhoff, J.F., 1985. *Rhodobacter veldkampii*, a new species of phototrophic purple nonsulfur bacteria. Int. J. Syst. Bacteriol. 35, 15–116.

Hansen, T., Sepers, A., van Gemerden, H., 1975. A new purple bacterium that oxidizes sulfide to extracellular sulfur and sulfate. Plant Soil 43, 17–27.

Holden-Dye, K., Crouch, L.I., Jones, M.R., 2008. Structure, function and interactions of the PufX protein. Biochim. Biophys. Acta 1777, 13–630.

Hsin, J., Chipot, C., Schulten, K., 2009a. A glycophorin A-like framework for the dimerization of photosynthetic core complexes. J. Am. Chem. Soc. 131, 17096–17098.

Hsin, J., Gumbart, J., Trabuco, L.G., Villa, E., Qian, P., Hunter, C.N., Schulten, K., 2009b. Protein-induced membrane curvature investigated through molecular dynamics flexible fitting. Biophys. J. 97, 321–329.

Hu, X., Ritz, T., Damjanovic, A., Autenrieth, F., Schulten, K., 2002. Photosynthetic apparatus of purple bacteria. Q. Rev. Biophys. 35, 1–62.

Hunter, C.N., Pennoyer, J.D., Sturgis, J.N., Farrelly, D., Niederman, R.A., 1988. Oligomerization states and associations of light-harvesting pigment–protein complexes of *Rhodobacter sphaeroides* as analyzed by lithium dodecyl sulfate-polyacrylamide gel electrophoresis. Biochemistry 27, 3459–3467.

Hunter, C.N., Tucker, J.D., Niederman, R.A., 2005. The assembly and organisation of photosynthetic membranes in *Rhodobacter sphaeroides*. Photochem. Photobiol. Sci. 4, 1023–1027.

Jamieson, S.J., Wang, P., Qian, P., Kirkland, J.Y., Conroy, M.J., Hunter, C.N., Bullough, P.A., 2002. Projection structure of the photosynthetic reaction centre-antenna complex of *Rhodospirillum rubrum* at 8.5 Å resolution. EMBO J. 21, 3927–3935.

Jarosławski, S., Duquesne, K., Sturgis, J.N., Scheuring, S., 2009. High-resolution architecture of the outer membrane of the Gram-negative bacteria *Roseobacter denitrificans*. Mol. Microbiol. 74, 1211–1222.

Jungas, C., Ranck, J.L., Rigaud, J.L., Joliot, P., Verméglio, A., 1999. Supramolecular organization of the photosynthetic apparatus of *Rhodobacter sphaeroides*. EMBO J. 18, 534–542.

Liu, L.N., Aartsma, T.J., Frese, R.N., 2008. Dimers of light-harvesting complex 2 from *Rhodobacter sphaeroides* characterized in reconstituted 2D crystals with atomic force microscopy. FEBS J. 275, 3157–3166.

Liu, L.N., Duquesne, K., Sturgis, J.N., Scheuring, S., 2009. Quinone pathways in entire photosynthetic chromatophores of *Rhodospirillum photometricum*. J. Mol. Biol. 393, 27–35.

Müller, D.J., Engel, A., 1999. Voltage and pH-induced channel closure of porin OmpF visualized by atomic force microscopy. J. Mol. Biol. 285, 1347–1351.

Oelze, J., Drews, G., 1972. Membranes of photosynthetic bacteria. Biochim. Biophys. Acta 265, 209–239.

Olsen, J.D., Tucker, J.D., Timney, J.A., Qian, P., Vassilev, C., Hunter, C.N., 2008. The organization of LH2 complexes in membranes from *Rhodobacter sphaeroides*. J. Biol. Chem. 283, 30772–30779.

Qian, P., Hunter, C.N., Bullough, P.A., 2005. The 8.5 Å projection structure of the core RC–LH1–PufX dimer of *Rhodobacter sphaeroides*. J. Mol. Biol. 349, 948–960.

Qian, P., Bullough, P.A., Hunter, C.N., 2008. Three-dimensional reconstruction of a membrane-bending complex: the RC–LH1–PufX core dimer of *Rhodobacter sphaeroides*. J. Biol. Chem. 283, 14002–14011.

Rasband, W.S., 1997–2005. ImageJ. U.S. National Institutes of Health, Bethesda, Maryland, USA. http://rsb.info.nih.gov/ij/.

Recchia, P.A., Davis, C.M., Lilburn, T.G., Beatty, J.T., Parkes-Loach, P.S., Hunter, C.N., Loach, P.A., 1998. Isolation of the PufX protein from *Rhodobacter capsulatus* and *Rhodobacter sphaeroides*: evidence for its interaction with the α-polypeptide of the core light-harvesting complex. Biochemistry 37, 11055–11063.

Roszak, A.W., Howard, T.D., Southall, J., Gardiner, A.T., Law, C.J., Isaacs, N.W., Cogdell, R.J., 2003. Crystal structure of the RC-LH1 core complex from *Rhodopseudomonas palustris*. Science 302, 1969–1972.

Saxton, W.O., Baumeister, W., 1982. The correlation averaging of a regularly arranged bacterial cell envelope protein. J. Microsc. 127, 127–138.

Schabert, F.A., Henn, C., Engel, A., 1995. Native *Escherichia coli* OmpF porin surfaces probed by atomic force microscopy. Science 268, 92–94.

Scheuring, S., 2006. AFM studies of the supramolecular assembly of bacterial photosynthetic core-complexes. Curr. Opinion Chem. Biol. 10, 387–393.

Scheuring, S., Sturgis, J.N., 2005. Chromatic adaptation of photosynthetic membranes. Science 309, 484–487.

Scheuring, S., Sturgis, J.N., 2009. Atomic force microscopy of the bacterial photosynthetic apparatus: plain pictures of an elaborate machinery. Photosynth. Res. 102, 197–211.

Scheuring, S., Seguin, J., Marco, S., Lévy, D., Robert, B., Rigaud, J.L., 2003a. Nanodissection and high-resolution imaging of the *Rhodopseudomonas viridis* photosynthetic core complex in native membranes by AFM. Proc. Natl. Acad. Sci. USA 100, 1690–1693.

Scheuring, S., Seguin, J., Marco, S., Lévy, D., Breyton, C., Robert, B., Rigaud, J.L., 2003b. AFM characterization of tilt and intrinsic flexibility of *Rhodobacter sphaeroides* light harvesting complex 2 (LH2). J. Mol. Biol. 325, 569–580.

Scheuring, S., Rigaud, J.L., Sturgis, J.N., 2004a. Variable LH2 stoichiometry and core clustering in native membranes of *Rhodospirillum photometricum*. EMBO J. 23, 4127–4133.

Scheuring, S., Sturgis, J.N., Prima, V., Bernadac, A., Lévy, D., Rigaud, J.L., 2004b. Watching the photosynthetic apparatus in native membranes. Proc. Natl. Acad. Sci. USA 101, 11293–11297.

Scheuring, S., Francia, F., Busselez, J., Melandri, B.A., Rigaud, J.L., Lévy, D., 2004c. Structural role of PufX in the dimerization of the photosynthetic core complex of *Rhodobacter sphaeroides*. J. Biol. Chem. 279, 3620–3626.

Scheuring, S., Busselez, J., Lévy, D., 2005. Structure of the dimeric PufX-containing core complex of *Rhodobacter blasticus* by in situ atomic force microscopy. J. Biol. Chem. 280, 1426–1431.

Scheuring, S., Gonçalves, R.P., Prima, V., Sturgis, J.N., 2006. The photosynthetic apparatus of *Rhodopseudomonas palustris*: structures and organization. J. Mol. Biol. 358, 83–96.

Scheuring, S., Boudier, T., Sturgis, J.N., 2007a. From high-resolution AFM topographs to atomic models of supramolecular assemblies. J. Struct. Biol. 159, 268–276.

Scheuring, S., Buzhynskyy, N., Jaroslawski, S., Gonçalves, R.P., Hite, R.K., Walz, T., 2007b. Structural models of the supramolecular organization of AQP0 and connexons in junctional microdomains. J. Struct. Biol. 160, 385–394.

Şener, M.K., Olsen, J.D., Hunter, C.N., Schulten, K., 2007. Atomic-level structural and functional model of a bacterial photosynthetic membrane vesicle. Proc. Natl. Acad. Sci. USA 104, 15723–15728.

Siebert, C.A., Qian, P., Fotiadis, D., Engel, A., Hunter, C.N., Bullough, P.A., 2004. Molecular architecture of photosynthetic membranes in *Rhodobacter sphaeroides*: the role of PufX. EMBO J. 23, 690–700.

Stark, W., Kuhlbrandt, W., Wildhaber, I., Wehrli, E., Muhlethaler, K., 1984. The structure of the photoreceptor unit of *Rhodopseudomonas viridis*. EMBO J. 3, 777–783.

Sturgis, J.N., Niederman, R.A., 2008. Atomic force microscopy reveals multiple patterns of antenna organization in purple bacteria: implications for energy transduction mechanisms and membrane modeling. Photosynth. Res. 95, 269–278.

Sturgis, J.N., Niedermann, R.A., 1996. The effect of different levels of the B800–850 light-harvesting complex on intracytoplasmic membrane development in Rhodobacter sphaeroides. Arch. Microbiol. 165, 235–242.

Sturgis, J.N., Tucker, J.D., Olsen, J.D., Hunter, C.N., Niederman, R.A., 2009. Atomic force microscopy studies of native photosynthetic membranes. Biochemistry 48, 3679–3698.

Tsukatani, Y., Matsuura, K., Masuda, S., Shimada, K., Hiraishi, A., Nagashima, K., 2004. Phylogenetic distribution of unusual triheme to tetraheme cytochrome subunit in the reaction center complex of purple photosynthetic bacteria. Photosynth. Res. 79, 83–91.

Tunnicliffe, R.B., Ratcliffe, E.C., Hunter, C.N., Williamson, M.P., 2006. The solution structure of the PufX polypeptide from *Rhodobacter sphaeroides*. FEBS Lett. 580, 6967–6971.

Walz, T., Jamieson, S.J., Bowers, C.M., Bullough, P.A., Hunter, C.N., 1998. Projection structures of three photosynthetic complexes from *Rhodobacter sphaeroides*: LH2 at 6 Å, LH1 and RC-LH1 at 25 Å. J. Mol. Biol. 282, 833–845.

Wang, Z.Y., Suzuki, H., Kobayashi, M., Nozawa, T., 2007. Solution structure of the *Rhodobacter sphaeroides* PufX membrane protein: implications for the quinone exchange and protein–protein interactions. Biochemistry 46, 3635–3642.

Weiss, M.S., Schulz, G.E., 1992. Structure of porin refined at 1.8 Å resolution. J. Mol. Biol. 227, 493–509.